Anna KRAWCZUK*, Jacek DOMIŃCZUK**

THE USE OF COMPUTER IMAGE ANALYSIS IN DETERMINING ADHESION PROPERTIES

Abstract

The paper discusses the use of computer image analysis in determining adhesion properties of materials, including the work of adhesion and surface free energy components. Also, it discusses methods and operators for edge detection employed in the determining of geometrical parameters which are then used as the basis for calculations. In addition, the paper presents an example of expanding the scope of investigations through the application of new IT solutions.

1. COMPUTER IMAGE PROCESSING AND METHODS OF IMAGE PROCESSING

Computer image analysis is currently used in numerous fields of science. This is an automatic method, which allows both the processing and analysis of images saved in digital form [1]. Until recently, adhesion properties were investigated with methods based on geometrical measurements carried out manually [2].

The development of computer technology has opened up new possibilities of analyzing recorded digital images. Also, the available image processing operations applicable in the analysis allow to improve the quality of images and to fully exploit information recorded in these images.

Current studies into adhesion properties are conducted by means of computer image analysis, which enables automatic measurement of a contact angle formed by a drop that is not reactive with a solid surface (Fig. 8) [3]. This measurement is particularly important in determining the work of adhesion and surface free energy.

---

* University of Life Sciences in Lublin, Department of Machine Operation and Management of Productive Process, ul. Głęboka 28, (81) 532 97 34, anna.krawczuk.up@gmail.com.
** Lublin University of Technology, Institute of Technological Information Systems ul. Nadbystrzycka 36, (81) 538 45 85, j.dominczuk@pollub.pl

The equations presented below (3, 4) show that the accuracy in determining the work of adhesion is related with precise measurement of a contact angle. The contact angle can be determined based on the measurements of geometrical dimensions of drops lying on a solid surface (Fig. 1). Having determined the dimensions of the drops, it is easy to calculate the contact angle with the formula:

$$tg\frac{\theta}{2} = \frac{k}{r}$$

(1)

The designations shown in Figure 1.

As for the drop shape shown in Figure 2, we can use the formula:

$$tg\frac{\theta}{2} = \frac{x}{r-h} = \sqrt{\frac{2h}{r-h}}$$

(2)

The designations shown in Figure 2.
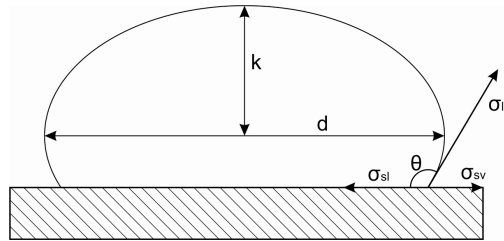
Fig. 1.Determination of the contact angle
by measuring the size of a drop [source: own study]
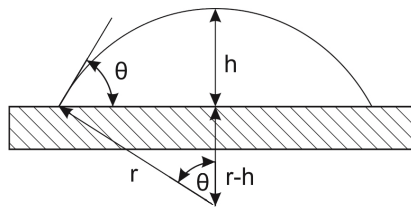
Fig. 2. Determination of the contact angle [source: own study]

Another method for determining the contact angle is to measure it directly. Performing a quantitative analysis of objects present in the images and taking geometrical measurements [2] is based on extracting elements, that is the detection of the contact angle's edges. On a monochrome image, the edge is a transition area between two levels of brightness, which is the line separating

the regions of different luminance [4]. Edge detection can both reduce the amount of data to analyze by filtering out less important pieces of information, while at the same time maintaining the properties of structures found in the images. Edge detection methods can be divided into two groups. The first group of methods studies the first derivative (gradient methods), while the second group is based on the study of the second derivative.

One of the fundamental methods for edge detection uses the first derivative of a function representing the change in a grayscale image along a set straight line. Due to the difficulty in determining the derivative, local gradients are adopted on the computer image as an approximation of the derivative. Based on the information about the rate of increase in the original data, the extremities of the first derivative of luminance are studied.

The second derivative of luminance shows the rate of change in the first derivative of luminance. The first derivative has a small value for images with inconspicuous transition between different areas of gray. In such cases, the second derivative is used, which assumes the value of zero for the edge.

We can distinguish the following operators in edge detection [5]:
a) operators of the first type – the Prewitt operator, Sobel operator and Roberts operator,
b) operators of the second type – Laplacian operators.

1.1. Roberts operator

The Roberts gradient is clearly directional. The differentiation of the two-dimensional function is performed along a certain direction; as for the Roberts gradient, this direction is located at 45 degrees [6]. The mask used by the Roberts operator is shown in Figure 3. It can also be written in the minimized form as a 2x2 mask.

$$\begin{bmatrix} 0 & 0 & 0 \\ -1 & 0 & 0 \\ 0 & 1 & 0 \end{bmatrix}$$

Fig. 3. Mask used by the Roberts operator [source: own study]

Depending on the mask form used, this gradient always highlights the lines of a set orientation.

1.2. Prewitt operator

This operator is used to detect vertical and horizontal edges in images. The mask used by the Prewitt operator is shown in Figure 4.

$$\begin{bmatrix} -1 & -1 & -1 \\ 0 & 0 & 0 \\ 1 & 1 & 1 \end{bmatrix}$$

Fig. 4. Mask used by the Prewitt operator [source: own study]

1.3. Sobel operator

The Sobel mask is a weight mask and has the form as shown in Figure 5. This mask enhances the influence of the nearest pixel environment when determining the value of a pixel on the resulting image.

$$\begin{bmatrix} -1 & -2 & -1 \\ 0 & 0 & 0 \\ 1 & 2 & 1 \end{bmatrix}$$

Fig. 5. Mask used by the Sobel operator [source: own study]

This mask can be rotated around its center point, which allows performing nine different filtration.

1.4. Laplacian operators

Roberts, Prewitt and Sobel masks define the edges only in eight directions. Often, the edges in images do not follow these directions. In order to detect edges of other directions and highlight the contours of objects in images, we use other masks – the so-called Laplacians.

A Laplacian operator is a combination of second partial derivatives of the input function. The maximum of the first derivative is the zero crossing point of the second derivative of the function. This point corresponds to the fastest changes in the function. The Laplacians are used to detect edges in images with no clear transition between the levels of gray. In this case, the first derivative has a low value and the second derivative is used to detect the edge (the second derivative of the edge assumes the 0 value). The most frequently used Laplacian masks are shown in Figure 6.

$$\begin{bmatrix} 0 & -1 & 0 \\ -1 & 4 & -1 \\ 0 & -1 & 0 \end{bmatrix} \begin{bmatrix} 0 & -1 & 0 \\ -1 & 5 & -1 \\ 0 & -1 & 0 \end{bmatrix} \begin{bmatrix} -1 & -1 & -1 \\ -1 & 8 & -1 \\ -1 & -1 & -1 \end{bmatrix}$$

$$\begin{bmatrix} 1 & -2 & 1 \\ -2 & 4 & -2 \\ 1 & -2 & 1 \end{bmatrix} \begin{bmatrix} 1 & -2 & 1 \\ -2 & 5 & -2 \\ 1 & -2 & 1 \end{bmatrix} \begin{bmatrix} -1 & -1 & -1 \\ -1 & 9 & -1 \\ -1 & -1 & -1 \end{bmatrix}$$

Fig. 6. Laplacian masks [source: own study]

2. MEASUREMENT PROCEDURE

The procedure for measuring the contact angle based on the computer image analysis is performed in the following steps:
1. Image acquisition and processing to digital form.
2. Edge detection of the measured drop.
3. Determination of the contact angle.

2.1. Image acquisition and processing to digital form

A schematic diagram of the measurement channel used for measuring the surface tension and determining adhesion properties of samples of solids is given in Figure 7. The sample is placed on a horizontal measuring table (1). Using a syringe (2), a drop of the measuring liquid with known parameters (3) is placed on the sample. The measuring table with the sample and the drop is illuminated by a focused light source (4). An image of the drop is recorded by a camera (5) and transferred directly to a computer where the contact angle is automatically measured with specialist software. The contact angle results are used to calculate such parameters as the work of adhesion and surface free energy. The analysis additionally determined other geometrical parameters of the analyzed image that can be used in the analysis of properties of the surface layer (Fig. 8).
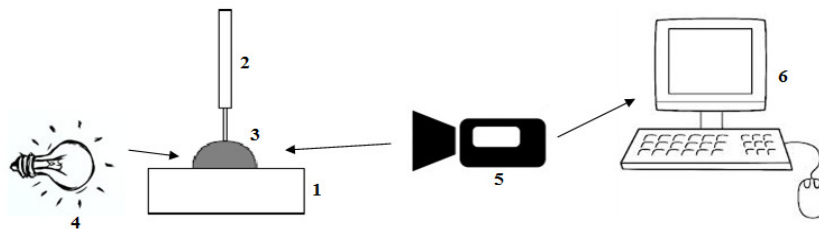
Fig. 7. Schematic diagram of the measurement channel [source: own study]

Prior to the measurements, it is necessary to prepare the device appropriately. The analysis and evaluation of a digital image considerably affects measurement precision. In order to receive an optimum image of the drop, it is necessary to adjust three image parameters: size, brightness and sharpness. An image is optimal if the drop is 2/3 width of the video image and its edges are sharp, without any interfering reflections. Also, the received mirror image of the drop must be clear. The lighting should be set such that a homogeneous lighter gray zone is above the baseline. The adjustments allow the precise determining of the baseline which is key to making measurements.

No.	Age [sec]	Theta(M)[deg]	IFT [mN/m]	Vol [ul]	Area [mm²]	BD [mm]	System	Theta(L)[deg]	Theta(R)[deg]	WoA [mN/m]
0-0	901.552	101.1 ± 0.81		3.41	8.73	2.187	Water (Ström)	100.3	101.9	58.84 ± 1.01
0-1	938.458	114.9 ± 0.31		5.59	12.56	2.172	Water (Ström)	115.2	114.6	42.15 ± 0.36
0-2	974.244	89.8 ± 0.24		3.43	8.72	2.398	Water (Ström)	90.0	89.5	73.07 ± 0.31
0-3	1002.634	94.7 ± 0.34		3.27	8.47	2.269	Water (Ström)	94.4	95.1	66.77 ± 0.43
0-4	1014.104	105.4 ± 0.60		4.99	11.24	2.323	Water (Ström)	104.8	106.0	53.47 ± 0.74
0-5	1023.921	89.2 ± 0.18		3.37	8.64	2.393	Water (Ström)	89.3	89.0	73.86 ± 0.23
0-6	1041.138	92.7 ± 0.47		3.51	8.87	2.358	Water (Ström)	92.3	93.2	69.34 ± 0.59
0-7	1052.331	93.3 ± 0.14		3.33	8.55	2.307	Water (Ström)	93.5	93.2	68.56 ± 0.17
0-8	1062.808	95.7 ± 0.15		3.57	8.97	2.318	Water (Ström)	95.5	95.8	65.63 ± 0.19
0-9	1072.941	112.8 ± 0.16		5.43	12.19	2.255	Water (Ström)	112.9	112.6	44.63 ± 0.19
0-M		99.0 ± 9.25		3.99 ±...	9.69 ± 1.63	2.298 ±...	Water (Ström)	98.8 ± 9.28	99.1 ± 9.24	61.63 ± 11.42
1-0	1447.388	115.2		5.91	12.91	2.298	Water (Ström)	115.3	115.2	41.77 ± 0.02
1-1	1447.895	102.6 ± 1.85		5.09	11.25	2.457	Water (Ström)	104.5	100.8	56.90 ± 2.30
1-2	1448.409	102.6 ± 1.92		5.10	11.27	2.458	Water (Ström)	104.6	100.7	56.88 ± 2.38
1-3	1448.915	102.7 ± 2.03		5.11	11.28	2.459	Water (Ström)	104.8	100.7	56.77 ± 2.51
1-4	1449.425	102.9 ± 2.09		5.12	11.29	2.459	Water (Ström)	105.0	100.8	56.57 ± 2.59
1-5	1449.925	102.6 ± 2.04		5.10	11.26	2.464	Water (Ström)	104.6	100.5	56.99 ± 2.53
1-6	1450.440	102.1 ± 1.97		5.06	11.21	2.473	Water (Ström)	104.1	100.2	57.49 ± 2.44
1-7	1450.940	102.4 ± 2.04		5.09	11.25	2.473	Water (Ström)	104.5	100.4	57.15 ± 2.53
1-8	1451.450	103.0 ± 2.14		5.15	11.33	2.470	Water (Ström)	105.1	100.8	56.47 ± 2.65
1-9	1451.956	102.9 ± 2.22		5.14	11.32	2.472	Water (Ström)	105.2	100.7	56.52 ± 2.74
1-10	1452.465	102.7 ± 2.27		5.13	11.29	2.476	Water (Ström)	104.9	100.4	56.86 ± 2.81
1-11	1452.970	103.0 ± 2.21		5.17	11.37	2.478	Water (Ström)	105.2	100.8	56.41 ± 2.74
1-12	1453.480	102.8 ± 2.22		5.15	11.33	2.485	Water (Ström)	105.0	100.6	56.68 ± 2.75
1-13	1453.980	102.9 ± 2.16		5.17	11.37	2.489	Water (Ström)	105.1	100.7	56.57 ± 2.68
1-14	1454.495	103.0 ± 2.28		5.16	11.35	2.489	Water (Ström)	105.3	100.7	56.44 ± 2.83
1-15	1454.995	103.0 ± 2.29		5.16	11.35	2.492	Water (Ström)	105.3	100.7	56.46 ± 2.84
1-16	1455.510	102.7 ± 2.29		5.14	11.32	2.497	Water (Ström)	105.0	100.4	56.85 ± 2.84
1-17	1456.011	102.7 ± 2.33		5.15	11.32	2.498	Water (Ström)	105.0	100.3	56.84 ± 2.88
1-18	1456.520	103.2 ± 2.47		5.19	11.38	2.494	Water (Ström)	105.7	100.7	56.21 ± 3.06
1-19	1457.025	103.1 ± 2.49		5.18	11.38	2.495	Water (Ström)	105.6	100.6	56.35 ± 3.08
1-20	1457.535	103.1 ± 2.52		5.18	11.37	2.495	Water (Ström)	105.6	100.6	56.29 ± 3.12
1-21	1458.035	102.6 ± 2.43		5.14	11.32	2.501	Water (Ström)	105.1	100.2	56.91 ± 3.02
1-22	1458.550	102.6 ± 2.49		5.14	11.31	2.501	Water (Ström)	105.1	100.1	56.92 ± 3.09
1-23	1459.050	102.7 ± 2.55		5.15	11.32	2.501	Water (Ström)	105.3	100.2	56.77 ± 3.16

[x ,y]: GrayVal   00:01:27

Fig. 8. View of the table automatically generated by the program for the analysis of surface layer properties [source: own study]

In this stage, the image analysis is performed in order to detect the drop's contour and the line separating the solid phase from the liquid phase. To this aim, different edge detection methods can be employed, such as the Sobel, Prewitt and Roberts methods, Laplacians and the Canny method [7]. The choice of the method depends on the quality of a received image.

2.2. Determination of the contact angle

Based on the detected edge, a theoretical drop profile is determined using the above described numerical method. Figure 9 shows the example of a droplet obtained in the measurements. The horizontal line is the baseline (the line which separates the solid from the measured drop), while the green line indicates the theoretical shape of the drop.

To determine the contact angle (which was then used to determine adhesion properties), we employed a measuring method in which the shape of a droplet is determined by the equation where the derivative at the point of intersection of the baseline with the line defining material surface creates an angle of inclination at the junction of three phases (contact angle).
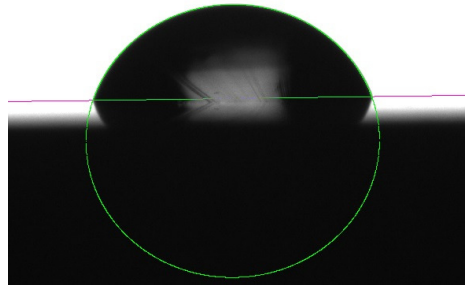
Fig. 9. Example of determining the baseline and drop contour
[source: own study]

3. INVESTIGATION OF ADHESION PROPERTIES

To calculate the surface free energy using contact angle measurements Young's equation is applied. This equation has the form [8]:

$$\sigma_{SV} = \sigma_{SL} + \sigma_{LV} \cos\theta_Y \tag{3}$$

where: σ_{SV} – the surface tension of the solid in equilibrium with saturated vapor of the liquid,

σ_{SL} – the interfacial surface tension of the solid and liquid,

σ_{LV} – the surface tension of the liquid in equilibrium with saturated vapor of the liquid,

$\cos\theta_Y$ – the angle formed by the tangent to the surface of the measured drop deposited on the surface of a solid at the contact point of three phases (equilibrium contact angle; Young's angle).

This equation was developed based on the condition of equilibrium of forces and can be described as "a simple relationship between the contact angle and surface tension of the liquid, surface tension of the solid and interfacial surface tension of the solid – liquid" [8]. Using the Gibbs theory, the equation can also be presented as (4). Based on the energy balance, we derive an equation for the three-phase equilibrium point (point A in Figure 10).

$$\gamma_{SV} = \gamma_{SL} + \gamma_{LV} \cos\theta_Y \tag{4}$$

where: γ_{SV} – the surface free energy of the solid in equilibrium with saturated vapor of the liquid,

γ_{SL} – the interfacial surface free energy of the solid and liquid,

γ_{LV} – the surface free energy of the liquid in equilibrium with saturated vapor of the liquid.

Young's equation is presented graphically in Figure 10.
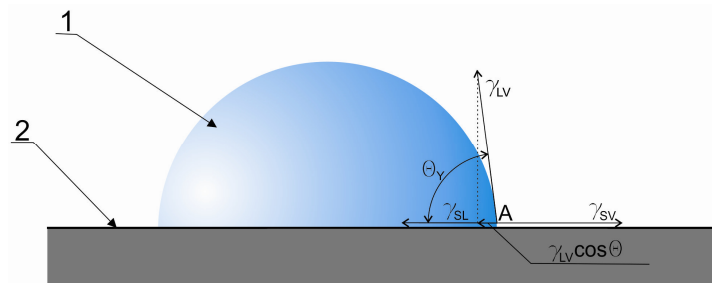
Fig. 10. Graphical presentation of Young's equation 1 – measured drop, 2 – tested material [8]

The use of Young's equation, which describes an ideal system, requires that fundamental conditions for taking measurements be observed. The surface on which measurements of the contact angle are taken should be, first, rigid enough to avoid deformation of the material under the influence of measured droplet and, second, suitably fixed to minimize drop deformation under vibration.

Another condition that must be met concerns suitable surface roughness, which is measured by an arithmetic average deviation of the roughness profile. This value should not exceed $0,5\mu$. The surface layer of the tested material should be free from any pollution; also it must be physically and chemically homogeneous, while the measuring liquids should be chemically neutral so as not to react with the material or material components.

As a result of the adoption of simplified assumptions, Equation (5) is obtained, which allows to determine the adhesion properties of a surface layer on the basis of the contact angle measurement results.

$$\gamma_S = \gamma_{SL} + \gamma_L \cos\theta \tag{5}$$

where: γ_S – the surface free energy of the solid,

γ_L – the surface free energy of the measuring liquid,

θ – the contact angle.

Surface free energy is often used to measure adhesive capacity of objects. The work of adhesion is defined as the work that is done against the forces of adhesion (the sum of all intermolecular interactions) during a reversible isothermal process to create a unit area of phases being in equilibrium [9]. The work of adhesion affects only intermolecular interactions. The work of adhesion for contact angles is calculated by the Dupre-Young equation. This equation has the form [8]:

$$W_a = \sigma_{LV}(1 + \cos\theta)$$ (6)

where: W_a – the work of adhesion.

Knowledge of the contact angle also allows to determine the polar and non-polar components of surface free energy using generally known computational methods [10].

4. CONCLUSIONS

Owing to the development of computer technology with regard to image analysis, current investigations of adhesive properties of surface layers allow better investigation of the effects of factors responsible for a given energy state. The possibility of determining exact values of such parameters as the work of adhesion and surface energy opens up new possibilities for the development of adhesive techniques based on the knowledge of energetic processes occurring on the surface of bonded materials. The possibility of performing image processing in real time also enables conducting studies that have so far been difficult to perform, such as taking measurements of the advancing contact angle, receding contact angle and dynamic contact angle [11].

As can be seen in Figure 11, due to its versatility the use of computer image analysis allows us to determine the parameters and characteristics that were impossible to determine with previous methods. Computer image analysis also allows to store information in the program integrated databases.
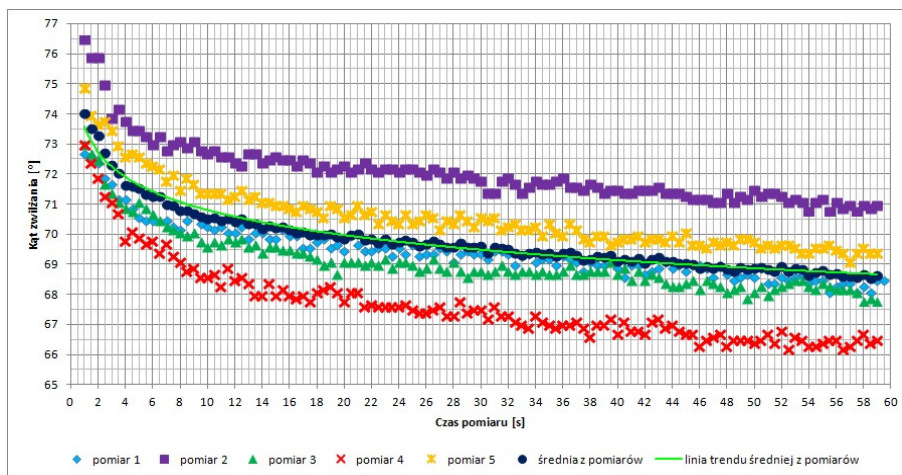
Fig. 11. Results of the dynamic contact angle measurements for polyamide PA6 after degreasing with the calculated average and indicated trend line [source: own study]

REFERENCES

[1]   ATAE-ALLAH et al.: *Measurement of surface tension and contact angle using entropic edge detection*. Measurement Science and Technology, volume 12, 2001, pp. 288-298.

[2]   DOMIŃCZUK J.: *Możliwości zastosowania systemu wizyjnego „MIKROSCAN" do pomiarów wielkości geometrycznych.* Eksploatacja i Niezawodność, nr 5, 2001, pp. 66-68.

[3]   DOMIŃCZUK J., KUCZMASZEWSKI J.: *Wybrane metody pomiaru pracy adhezji z wykorzystaniem komputerowej analizy obrazu*. III Ogólnopolska Konferencja Naukowo-Techniczna "POSTĘPY'99", Kraków, 1999.

[4]   KOPROWSKI R., WRÓBEL Z.: *Przetwarzanie obrazu w programie MATLAB.* wydanie I, Wydawnictwo Uniwersytetu Śląskiego, Katowice, 2001.

[5]   AGGARWAL H., MAINI R.: *Study and Comparison of Various Image Edge Detection Techniques.* International Journal of Image Processing*,* volume 3, 2009, pp. 1-12.

[6]   KOROHODA P., TADEUSIEWICZ R.: *Komputerowa analiza i przetwarzanie obrazów.*, Wydawnictwo Fundacji Postępu Telekomunikacji, Kraków, 1997.

[7]   AMIRFAZIL A., FARSHID CHINI S.: *A method for measuring contact angle of asymmetric and symmetric drops.* Colloids and Surfaces A: Physicochemical and Engineering Aspects, 388, 2011, pp. 29-37.

[8]   ŻENKIEWICZ M.: *Adhezja i modyfikowanie warstwy wierzchniej tworzyw wielkocząsteczkowych*. Wydawnictwo Naukowo Techniczne, Warszawa 2000.

[9]   ŻENKIEWICZ M.: *New method of analysis of the surface free energy of polymeric materials calculated with Owens-Wendt and Neumann methods*. Polimery, nr 7-8, 2006, pp. 584-587.

[10]   ŻENKIEWICZ M.: *Methods for the calculation of surface free energy of solids.* Journal of Achievements in Materials and Manufacturing Engineerig vol. 24, no. 1, 2007, pp. 137-145.

[11]   DUNCAN B. et al.: *Techniques for characterizing the wetting, coating and spreading of adhesive on surfaces*. NPL Report DEPC-MPR-020, 2005.